# **Author Index of Vol. 142**

Annavarapu, S., 261	
Apelian, D., 261	
Ayers, J. D., 221	
Babu, S. S., 209	
Baker, T. N., 115	
Beevers, C. J., 183	

Beevers, C. J., 183 Bhadeshia, H. K. D. H., 209 Bradt, R. C., 51

Chan, S. L.-I., 193 Chatterjee, A., 235 Cheng, P. C., 135 Copper, K. P., 221

Degallaix, S., 169

Feng, C. R., 221 Fine, M. E., 177

Gopalan, P., 11 Goya, M., 163 Grujicic, M., 255

Healy, J. C., 183 Hirth, J. P., 235 Hoagland, R. G., 235 Hong, S. I., 1 Huang, W.-S., 41

Ito, T., 203

Karmazin, L., 71 Kettunen, P., 125 Kim, G.-H., 177 Kim, H.-K., 145 Klauzner, A., 135 Kojima, H., 245 Kong, Q. P., 157 Krishnan, K. N., 79 Kwon, I.-B., 177

Laird, C., 1 Lawley, A., 261 Lee, H.-L., 193 Lee, S.-L., 41 Levi, C. G., 277 Li, H., 51 Li, J. C. M., 35 Locci, I. E., 221 Lucas, G. E., 277

Magnin, T., 169 Makel, D. D., 107 Maki, T., 63 Makita, A., 245 Malzahn Kampe, J. C., 221 Margolin, H., 11 Mathur, P., 261 Matsuzaki, Y., 63 Mohamed, F. A., 145

Mridha, S., 115

Nagaki, S., 163 Nagorka, M. S., 277

Prasad Rao, K., 79

Ridder, S. D., 277 Rios, P. R., 87 Ruuskanen, P., 125

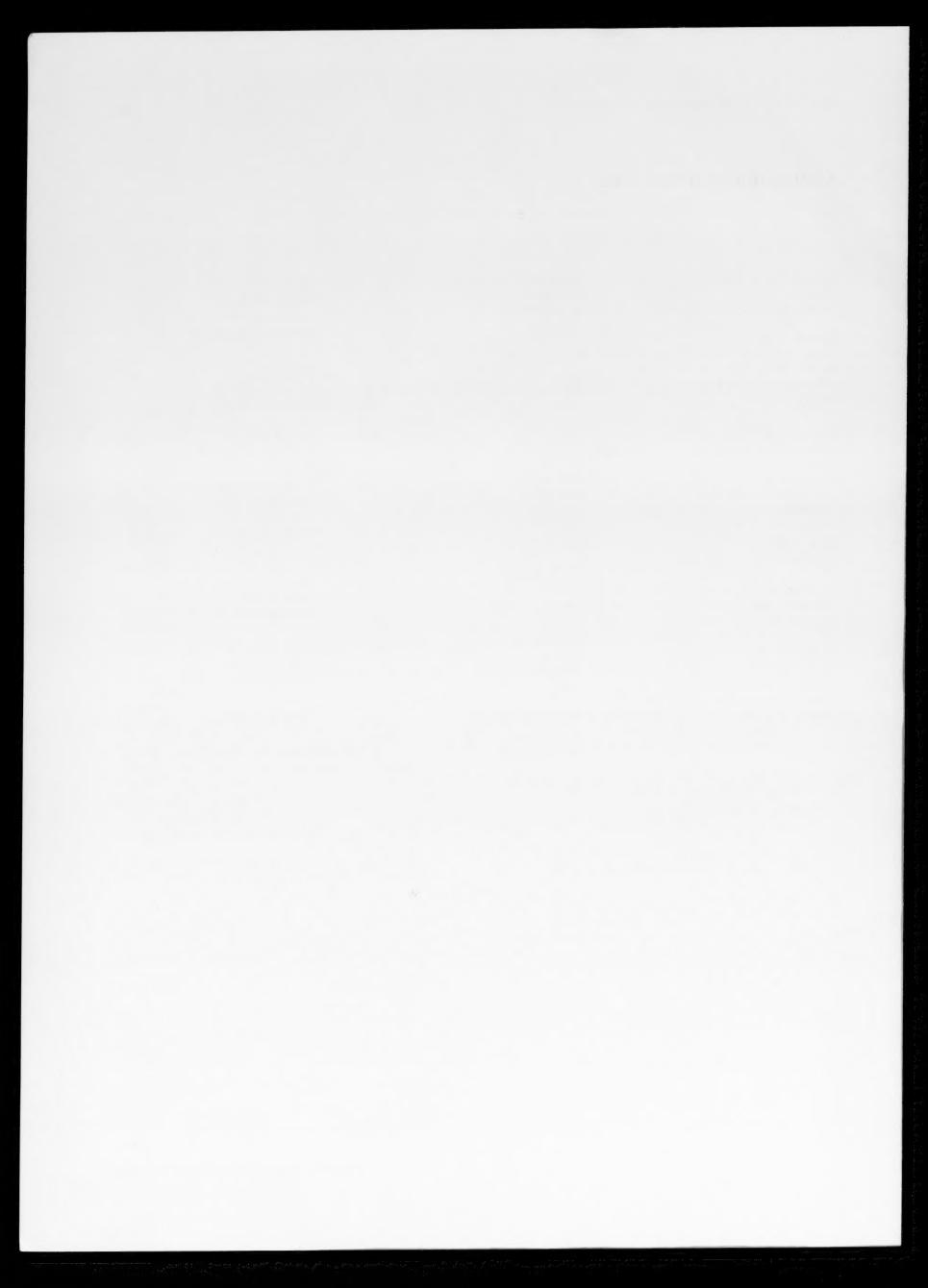
Samuel, F. H., 95 Shinozaki, D. M., 135 Shiue, S.-T., 41 Soussan, A., 169 Sowerby, R., 163

Takano, S., 245 Takegawa, Y., 203 Tamura, I., 63 Tangrila, S., 255 Tsuji, K., 203 Tsuzaki, K., 63

Wang, D. N., 157 Wang, Z. G., 25 Wilsdorf, H. G. F., 107

Yang, Z. A., 25

Zhang, T.-Y., 35



# Subject Index of Vol. 142

Aging

fatigue deformation accompanying dynamic strain aging in a pearlitic eutectoid steel, 63

Allovs

a study of fatigue crack growth in a particulate-reinforced Al-Si alloy at 23 and 220 °C, 183

characteristic features of laser-nitrided surfaces of two titanium alloys, 115

cyclic creep behaviour of a nickel-based alloy under different types of fracture, 157

cyclic hardening behavior of polycrystalline Cu-16at.%Al alloy, 1

effect of stress reduction ratio on the creep behavior of an Al-5wt.%Ag alloy, 145

experimental study of the austenitization process of hypereutectoid steel alloyed with small amounts of silicon, manganese and chromium, and with an initial structure of globular cementite in a ferrite matrix, 71

microstructural evaluation and thermal stability in rapidly solidified high-chromium-containing copper alloys, 221 phase transformation property of Ni-Ti-Cu alloy coil

under an applied stress, 203

the potential of rapid solidification in oxide-dispersionstrengthened copper alloy development, 277

work-hardening behaviour of nitrogen-alloyed austenitic stainless steels, 169

Aluminium

a study of fatigue crack growth in a particulate-reinforced Al-Si alloy at 23 and 220 °C, 183

cyclic-hardening behavior of polycrystalline Cu-16at.%Al allov, 1

effect of frequency on cyclic creep of polycrystalline aluminium at room temperature, 25

effect of stress reduction ratio on the creep behavior of an Al-5wt.%Ag alloy, 145

Amplitude spectrum

effect of cyclic straining on the harmonic amplitude spectrum of magnetoelastically generated voltage  $u_{\rm B}$ , 125

Austenite

experimental study of the austenitization process of hypereutectoid steel alloyed with small amounts of silicon, manganese and chromium, and with an initial structure of globular cementite in a ferrite matrix, 71

work-hardening behaviour of nitrogen-alloyed austenitic stainless steels, 169

Boron

effects of hydrogen pre-charging for quenched-andtempered AISI 1520 steels containing boron, 235

Knoop microhardness anisotropy of single-crystal LaB<sub>6</sub>, 51

Carbon

method for the determination of mole fraction and com-

position of a multicomponent f.c.c. carbonitride, 87

recrystallization behaviour of a C-Mn steel, a titaniuminterstitial-free steel and a niobium-microalloyed steel during strip rolling, 95

Chromium

experimental study of the austenitization process of hypereutectoid steel alloyed with small amounts of silicon, manganese and chromium, and with an initial structure of globular cementite in a ferrite matrix, 71

microstructural evolution and thermal stability in rapidly solidified high-chromium-containing copper alloys, 221

Copper

cyclic-hardening behavior of polycrystalline Cu-16at.%Al alloy, 1

inelastic deformation of polyimide-copper thin films, 135 microstructural evolution and thermal stability in rapidly solidified high-chromium-containing copper alloys, 221 phase transformation property of Ni-Ti-Cu alloy coil under an applied stress, 203

the influence of loading methods on fatigue crack initiation in polycrystalline copper at ambient temperature, 177

the potential of rapid solidification in oxide-dispersionstrengthened copper alloy development, 277

Corrosion

effect of microstructure on stress corrosion cracking behaviour of austenitic stainless steel weld metals, 79

Crack

a study of fatigue crack growth in a particulate-reinforced Al-Si alloy at 23 and 220 °C, 183

the influence of loading methods on fatigue crack initiation in polycrystalline copper at ambient temperature, 177

Cracking

effect of microstructure on stress corrosion cracking behaviour of austenitic stainless steel weld metals, 79

elastic interaction between screw dislocations and a blunting interfacial crack, 41

elastic stresses, twin boundaries and fatigue cracking, 11 image forces and shielding effects of a screw dislocation near a finite-length crack, 35

Creep

cyclic creep behaviour of a nickel-based alloy under different types of fracture, 157

effect of frequency on cyclic creep of polycrystalline aluminium at room temperature, 25

effect of stress reduction ratio on the creep behavior of an Al-5wt.%Ag alloy, 145

Crystallography

a direct study of grain boundary allotriomorphic ferrite crystallography, 209

Crystals

Knoop microhardness anisotropy of single-crystal LaB<sub>6</sub>, 51

stress-induced  $\alpha \rightarrow \beta$  transformation of V<sub>2</sub>H and V<sub>2</sub>D and growth of  $\beta$  single-domain crystals, 245

#### Deformation

fatigue deformation accompanying dynamic strain aging in a pearlitic eutectoid steel, 63

inelastic deformation of polyimide-copper thin films, 135

#### **Fatigue**

a study of fatigue crack growth in a particulate-reinforced Al-Si alloy at 23 and 220 °C, 183

elastic stresses, twin boundaries and fatigue cracking, 11 fatigue deformation accompanying dynamic strain aging in a pearlitic eutectoid steel, 63

the influence of loading methods on fatigue crack initiation in polycrystalline copper at ambient temperature, 177

### **Ferrite**

a direct study of grain boundary allotriomorphic ferrite crystallography, 209

#### Ferrite bands

hydrogen embrittlement of AISI 4130 steel with an alternate ferrite/pearlite banded structure, 193

#### Fracture

cyclic creep behaviour of a nickel-based alloy under different types of fracture, 157

#### Grain boundaries

a direct study of grain boundary allotriomorphic ferrite crystallography, 209

### Hardening

cyclic-hardening behavior of polycrystalline Cu-16at.%Al alloy, 1

#### Hydrogen

effects of hydrogen pre-charging for quenched-andtempered AISI 1520 steels containing boron, 235

hydrogen embrittlement of AISI 4130 steel with an alternate ferrite/pearlite banded structure, 193

### Image forces

image forces and shielding effects of a screw dislocation near a finite-length crack, 35

## Kinetic analysis

thermodynamic and kinetic analyses of time-temperature-sensitization diagrams in austenitic stainless steels, 255

#### Lanthanum

Knoop microhardness anisotropy of single-crystal LaB<sub>6</sub>, 51

#### Lasers

characteristic features of laser-nitrided surfaces of two titanium alloys, 115

## Localized melting

localized melting at separation of AISI 4340 steel tensile samples, 107

#### Magnetization

effect of cyclic straining on the harmonic amplitude spectrum of magnetoelastically generated voltage  $u_B$ , 125

## Manganese

experimental study of the austenitization process of hypereutectoid steel alloyed with small amounts of silicon, manganese and chromium, and with an initial structure of globular cementite in a ferrite matrix, 71 recrystallization behaviour of a C-Mn steel, a titaniuminterstitial-free steel and a niobium-microalloyed steel during strip rolling, 95

#### Mole fraction

method for the determination of mole fraction and composition of a multicomponent f.c.c. carbonitride, 87

#### Nickel

cyclic creep behaviour of a nickel-based alloy under different types of fracture, 157

phase transformation property of Ni-Ti-Cu alloy coil under an applied stress, 203

#### Niobiun

recrystallization behaviour of a C-Mn steel, a titaniuminterstitial-free steel and a niobium-microalloyed steel during strip rolling, 95

#### Nitrogen

characteristic features of laser nitrided surfaces of two titanium alloys, 115

method for the determination of mole fraction and composition of a multicomponent f.c.c. carbonitride, 87

work-hardening behaviour of nitrogen-alloyed austenitic stainless steels, 169

## Oxygen

the potential of rapid solidification in oxide-dispersionstrengthened copper alloy development, 277

#### Pearlite bands

hydrogen embrittlement of AISI 4130 steel with an alternate ferrite/pearlite banded structure, 193

## Phase transformations

phase transformation property of Ni-Ti-Cu alloy coil under an applied stress, 203

#### Polycrystals

cyclic-hardening behavior of polycrystalline Cu-16at.%Al alloy, 1

effect of frequency on cyclic creep of polycrystalline aluminium at room temperature, 25

### Polyimide

inelastic deformation of polyimide-copper thin films, 135 Porous metals

an anisotropic yield function for porous metal, 163

## Quenched steels

effects of hydrogen pre-charging for quenched-andtempered AISI 1520 steels containing boron, 235

#### Rapid solidification

the potential of rapid solidification in oxide-dispersionstrengthened copper alloy development, 277

# Screw dislocations

elastic interaction between screw dislocations and a blunting interfacial crack, 41

image forces and shielding effects of a screw dislocation near a finite-length crack, 35

## Shielding effects

image forces and shielding effects of a screw dislocation near a finite-length crack, 35

#### Silicor

a study of fatigue crack growth in a particulate-reinforced Al-Si alloy at 23 and 220 °C, 183

experimental study of the austenitization process of hypereutectoid steel alloyed with small amounts of silicon, manganese and chromium, and with an initial structure of globular cementite in a ferrite matrix, 71

Silver

effect of stress reduction ratio on the creep behavior of an Al-5wt.%Ag alloy, 145

Spray casting

spray casting: an integral model for process understanding and control, 261

Stainless steels

thermodynamic and kinetic analyses of time-temperature-sensitization diagrams of austenitic stainless steels, 255

work-hardening behaviour of nitrogen-alloyed austenitic stainless steels, 169

Steel

recrystallization behaviour of a C-Mn steel, a titaniuminterstitial-free steel and a niobium-microalloyed steel during strip rolling, 95

Steels

effect of microstructure on stress corrosion cracking behaviour of austenitic stainless steel weld metals, 79

effects of hydrogen pre-charging for quenched-andtempered AISI 1520 steels containing boron, 235

experimental study of the austenitization process of hypereutectoid steel alloyed with small amounts of silicon, manganese and chromium, and with an initial structure of globular cementite in a ferrite matrix, 71

fatigue deformation accompanying dynamic strain aging in a pearlitic eutectoid steel, 63

hydrogen embrittlement of AISI 4130 steel with an alternate ferrite/pearlite banded structure, 193

localized melting at separation of AISI 4340 steel tensile samples, 107

thermodynamic and kinetic analyses of time-temperature-sensitization diagrams in austenitic stainless steels, 255

work-hardening behaviour of nitrogen-alloyed austenitic stainless steels, 169

Strain

effect of cyclic straining on the harmonic amplitude spectrum of magnetoelastically generated voltage  $u_{\rm B}$ , 125

fatigue deformation accompanying dynamic strain aging in a pearlitic eutectoid steel, 63

Stress

effect of microstructure on stress corrosion cracking behaviour of austenitic stainless steel weld metals, 79

effect of stress reduction ratio on the creep behavior of an Al-5wt.%Ag alloy, 145

elastic stresses, twin boundaries and fatigue cracking, 11 phase transformation property of Ni-Ti-Cu alloy coil under an applied stress, 203

stress-induced  $\alpha \rightarrow \beta$  transformation of V<sub>2</sub>H and V<sub>2</sub>D and growth of  $\beta$  single-domain crystals, 245

Strip rolling

recrystallization behaviour of a C-Mn steel, a titaniuminterstitial-free steel and a niobium-microalloyed steel during strip rolling, 95

Tempered steels

effects of hydrogen pre-charging for quenched-andtempered AISI 1520 steels containing boron, 235

Thermal stability

microstructural evolution and thermal stability in rapidly solidified high-chromium-containing copper alloys, 221

Thermodynamic analysis

thermodynamic and kinetic analyses of time-temperature-sensitization diagrams in austenitic stainless steels, 255

Thin films

inelastic deformation of polyimide-copper thin films, 135 litanium

characteristic features of laser-nitrided surfaces of two titanium alloys, 115

phase transformation property of Ni-Ti-Cu alloy coil under an applied stress, 203

recrystallization behaviour of a C-Mn steel, a titaniuminterstitial-free steel and a niobium-microalloyed steel during strip rolling, 95

Weld metals

effect of microstructure on stress corrosion cracking behaviour of austenitic stainless steel weld metals, 79

Yield functions

an anisotropic yield function for porous metal, 163

